

ARTICLE

Received 2 Mar 2015 | Accepted 19 Jun 2015 | Published 28 Jul 2015

DOI: 10.1038/ncomms8870

OPEN

Mutations in *CDCA7* and *HELLS* cause immunodeficiency-centromeric instability-facial anomalies syndrome

Peter E. Thijssen¹, Yuya Ito², Giacomo Grillo³, Jun Wang^{1,†}, Guillaume Velasco³, Hirohisa Nitta², Motoko Unoki², Minako Yoshihara⁴, Mikita Suyama⁴, Yu Sun^{1,†}, Richard J.L.F. Lemmers¹, Jessica C. de Greef¹, Andrew Gennerly^{5,6}, Paolo Picco⁷, Barbara Kloeckener-Gruissem^{8,9}, Tayfun Güngör¹⁰, Ismail Reisli¹¹, Capucine Picard^{12,13,14,15,16,17}, Kamila Kebaili¹⁸, Bertrand Roquelaure¹⁹, Tsuyako Iwai²⁰, Ikuko Kondo²¹, Takeo Kubota²², Monique M. van Ostaijen-Ten Dam²³, Maarten J.D. van Tol²³, Corry Weemaes²⁴, Claire Francastel³, Silvère M. van der Maarel¹ & Hiroyuki Sasaki²

The life-threatening Immunodeficiency, Centromeric Instability and Facial Anomalies (ICF) syndrome is a genetically heterogeneous autosomal recessive disorder. Twenty percent of patients cannot be explained by mutations in the known ICF genes DNA methyltransferase 3B or zinc-finger and BTB domain containing 24. Here we report mutations in the cell division cycle associated 7 and the helicase, lymphoid-specific genes in 10 unexplained ICF cases. Our data highlight the genetic heterogeneity of ICF syndrome; however, they provide evidence that all genes act in common or converging pathways leading to the ICF phenotype.

¹ Department of Human Genetics, Leiden University Medical Center, Leiden 2333ZA, The Netherlands. ² Division of Epigenomics and Development, Department of Molecular Genetics, Medical Institute of Bioregulation, Kyushu University, Fukuoka 812-8582, Japan. ³ CNRS UMR7216, Epigenetics and Cell Fate, Université Paris Diderot, Sorbonne Paris Cité, 75205 Paris, France. ⁴ Division of Bioinformatics, Department of Multi-scale Research Center for Medical Science, Medical Institute of Bioregulation, Kyushu University, Fukuoka 812-8582, Japan. ⁵ Department of Paediatric Immunology, Newcastle Upon Tyne Hospital, NHS Foundation Trust, Newcastle Upon Tyne, UK. ⁶ Institute of Cellular Medicine, Newcastle University, Newcastle Upon Tyne NE1 4LP, UK. ⁷ Division of Pediatrics and Pediatric Rheumatology, G. Gaslini Scientific Institute, Genova 16147, Italy. ⁸ Institute of Medical Molecular Genetics, University of Zurich, Schlieren 8952, Switzerland. ⁹ Department of Biology, ETH Zurich, Zurich 8093, Switzerland. ¹⁰ Department of Oncology, University Children's Hospital, Zurich 8032, Switzerland. ¹¹ Department of Pediatric Immunology and Allergy, Necmettin Erbakan University, Meram Medical Faculty, Konya 42080, Turkey. ¹² Centre de Référence Déficits Immunitaires Héritaires, AP-HP, 75743 Paris, France. ¹³ Centre d'Etude des Déficits Immunitaires, Hôpital Universitaire Necker-Enfants Malades, AP-HP, 75743 Paris, France. ¹⁴ Laboratoire de Génétique Humaine des Maladies Infectieuses, Inserm, 75743, Paris, France. ¹⁵ Université Paris Descartes, Institut Imagine, Sorbonne Paris, 75743 Paris, France. ¹⁶ Unité d'immunologie et d'hématologie pédiatrique, Hôpital Necker-Enfants Malades, 75743, Paris, France. ¹⁷ Inserm UMR 768, 75015 Paris, France. ¹⁸ Centre de Référence Déficits Immunitaires Héritaires, Institut d'Hématologie et d'Oncologie Pédiatrique, CHU de Lyon, 69008 Lyon, France. ¹⁹ Service d'hépto-gastro-entérologie et nutrition, endocrinologie et néphrologie pédiatriques, Hôpital de la Timone, CHU Marseille, 13385 Marseille, France. ²⁰ Department of Pediatric Hematology and Oncology, Shikoku Medical Center for Children and adults, Kagawa 765-8507, Japan. ²¹ Department of Pediatrics, Oida Hospital, Kochi 788-0001, Japan. ²² Department of Epigenetic Medicine, Faculty of Medicine, Interdisciplinary Graduate School of Medicine and Engineering, University of Yamanashi, Yamanashi 409-3898, Japan. ²³ Department of Pediatrics, Laboratory for Immunology, Leiden University Medical Center, Leiden 2333ZA, The Netherlands. ²⁴ Department of Pediatric Infectious Diseases and Immunology, Radboud University Nijmegen Medical Center, Nijmegen 6500HC, The Netherlands. † Present address: Institutes of Biology and Medical Sciences, Soochow University, Suzhou 215123, China (J.W.); Shanghai Institute for Pediatric Research, Xin Hua Hospital, Shanghai Jiao Tong University School of Medicine, Shanghai, China (Y.S.). Correspondence and requests for materials should be addressed to C.F. (email: claire.francastel@univ-paris-diderot.fr) or to S.M. (email: Maarel@lumc.nl) or to H.S. (email: hsasaki@bioreg.kyushu-u.ac.jp).

Immunodeficiency, Centromeric Instability and Facial Anomalies (ICF) syndrome is characterized by recurrent and often fatal respiratory and gastrointestinal infections as a consequence of hypo- or a-gammaglobulinemia in the presence of B cells^{1,2}. Nearly all patients also present with distinct facial anomalies, including hypertelorism, flat nasal bridge and epicanthus^{1,2}. Centromeric instability is the cytogenetic hallmark of ICF syndrome. It involves the juxtacentromeric heterochromatin repeats on chromosomes 1, 9 and 16 and is comparable to what is observed after treatment of cells with demethylating agents^{3,4}. Therefore, CpG hypomethylation of juxtacentromeric satellite types II and III is a diagnostic for ICF syndrome, with additional hypomethylation of centromeric α -satellite repeats in *DNMT3B* mutation-negative patients^{5,6}.

Mutations in the DNA methyltransferase 3B (*DNMT3B*) gene (OMIM 602900; ICF1) account for ~50% of ICF cases, while ~30% of cases have mutations in the zinc-finger and BTB domain containing 24 (*ZBTB24*) gene (OMIM 614064; ICF2)^{2,5}. *DNMT3B* is a *de novo* DNA methyltransferase, primarily acting during early development with a preference for CpG dense regions⁷. ICF1 mutations in the catalytic domain of *DNMT3B* result in largely reduced methyltransferase activity^{8,9}. The function of *ZBTB24* is unknown, but it belongs to a family of ZBTB proteins of which many have regulatory roles in haematopoietic differentiation^{10,11}. Despite the successful identification of ICF genes, the pathophysiological mechanism underlying the syndrome remains largely unresolved.

Previous studies indicated further genetic heterogeneity in ICF syndrome². To identify the genetic cause in genetically unexplained cases (ICFX), we combined homozygosity mapping with whole-exome sequencing. By using an autosomal recessive inheritance model and prioritizing homozygous variants in consanguineous families, we now identify four different homozygous and potentially damaging variants in the cell division cycle associated 7 (*CDCA7*) gene in five ICFX patients (now referred to as ICF3). In an additional five ICFX patients, we identify compound heterozygous and homozygous variants in the helicase, lymphoid-specific (*HELLS*) gene (ICF4). We show that knockdown of both new ICF genes leads to hypomethylation of juxtacentromeric heterochromatin repeats in a murine cell model. Our results emphasize the genetic heterogeneity of ICF syndrome, nonetheless providing evidence that all four ICF genes are involved in at least one common pathway.

Results

Missense mutations in *CDCA7* cause ICF syndrome type 3. We selected 13 ICFX patients from 11 families, negative for mutations in *DNMT3B* or *ZBTB24*, of whom the clinicopathological characteristics are listed in Supplementary Table 1. Hypomethylation of pericentromeric satellite type II (Sat II), common to all ICF patients, and centromeric α -satellite DNA repeats, shown to be affected only in ICF2 and ICFX, was shown before for a subset of patients^{2,5,6,12}. For an additional set of ICFX patients, we

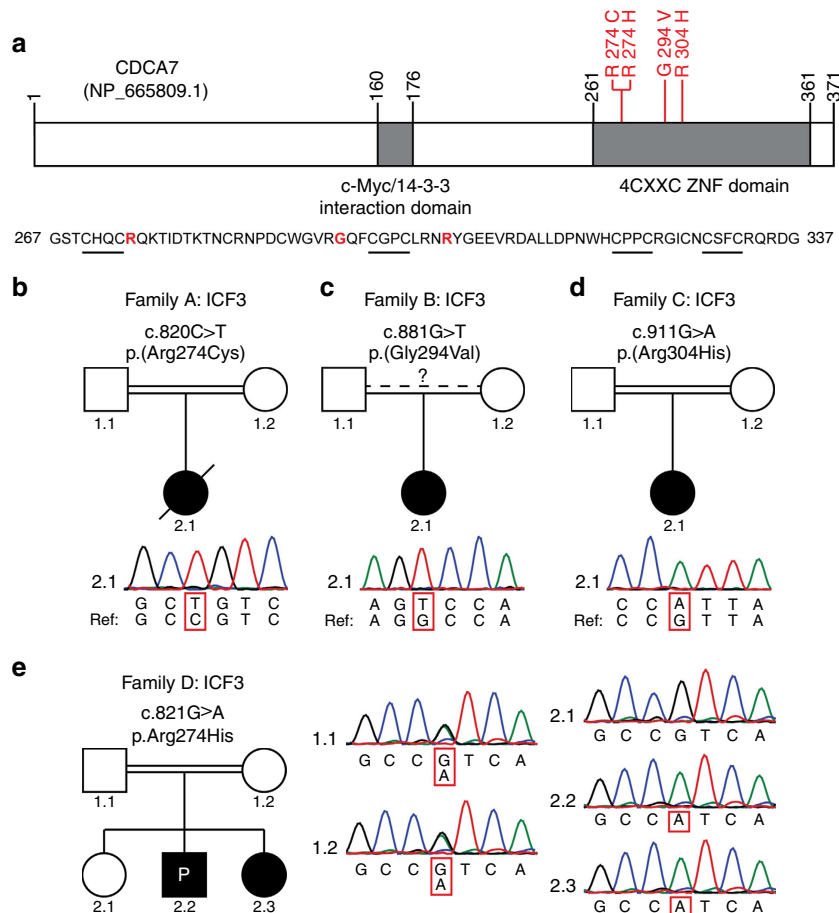


Figure 1 | Homozygous missense mutations in *CDCA7* in five ICF3 patients. (a) Schematic representation of *CDCA7*, with the identified homozygous missense mutations in red. Sequence outtake: 4-CXXC-type zinc-finger domain, CXXC motifs are underlined, mutated residues in red. (b–d) Sanger sequencing confirmation of missense mutations in *CDCA7* in families A–C. All variants were homozygous, the reference sequence is displayed for comparison. (e) Sanger sequencing confirmation of the homozygous missense *CDCA7* mutation in patients 2.2 (proband) and 2.3 of family D. Both parents are heterozygous for the variant, sibling 2.1 is unaffected and homozygous for the wild-type (wt) allele.

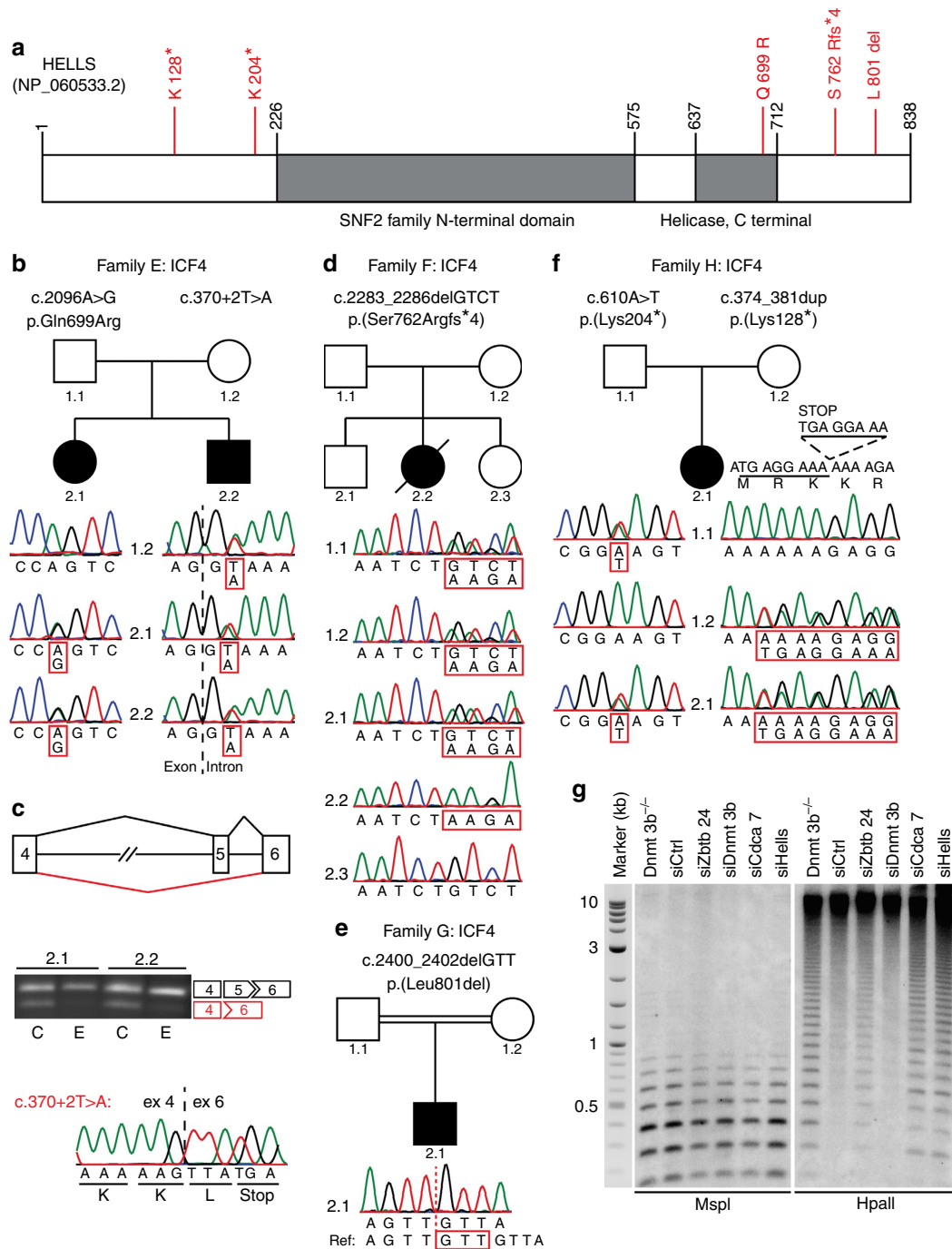


Figure 2 | Mutations in *HELLS* in five ICF4 patients. (a) Schematic representation of *HELLS*, with the identified mutations in red. (b) Sanger sequencing confirmation of *HELLS* mutations in family E. Only c.370 + 2T > A was identified in maternal DNA, indicating different allelic origins of both mutations, or *de novo* occurrence of the second mutation. (c) RT-PCR analysis of *HELLS* mRNA on treatment of patient-derived fibroblasts with cycloheximide (C) revealed that c.370 + 2T > A leads to complete skipping of exon 5 and disruption of the open reading frame. Ethanol-treated samples (E) served as controls, alternative splicing was confirmed using Sanger’s sequencing in two independent experiments for both samples. (d) Sanger sequencing confirmation of a homozygous out-of-frame deletion in *HELLS* in family F. Both parents as well as unaffected sibling 2.1 are heterozygous for the deletion allele; unaffected sibling 2.3 is homozygous for the wt allele. (e) Sanger sequencing confirmation of a homozygous in-frame deletion in *HELLS* in family G. Both parents are heterozygous for the deletion allele. (f) Sanger sequencing confirmation of nonsense mutations in *HELLS* in family H. Different allelic origin was confirmed in parental DNA. (g) Southern blot analysis of minor satellite DNA methylation in *Dnmt3b*^{-/-} and siRNA-treated wt MEFs after digesting DNA with *MspI* or its methylation-sensitive isoschizomer *HpaII* revealed CpG hypomethylation on knockdown of *Zbtb24*, *Cdca7* and *Hells*. Molecular weights of the 2-Log DNA size marker are in kilobasepairs.

confirmed Sat II and α -satellite hypomethylation using Southern blot analysis (Supplementary Fig. 1). In five ICFX patients from four families we identified and confirmed homozygous missense mutations in *CDCA7*, all near the first two zinc-finger motifs in

the conserved carboxyterminal 4-CXXC-type zinc-finger domain (Fig. 1a–e). Segregation with disease was confirmed in family D and all mutations were predicted to be pathogenic and have an allele frequency supporting pathogenicity (Fig. 1e, Supplementary

Table 1). *CDCA7* is involved in neoplastic transformation, *MYC*-dependent apoptosis and haematopoietic stem cell emergence; however, its molecular function is unknown^{13,14}. All four zinc-finger motifs are completely conserved in the highly homologous 4-CXXC zinc-finger domain of the transcriptional repressor *CDCA7-Like* (*CDCA7L*; Supplementary Fig. 2). The repressive activity of *CDCA7L* is dependent on its 4-CXXC domain, and by homology *CDCA7* mutations in ICF3 may disrupt a similar function¹⁵.

Mutations in HELLS cause ICF syndrome type 4. In an additional five ICFX patients from four families, we identified mutations in *HELLS* that were predicted to be pathogenic and with allele frequencies supporting pathogenicity (Fig. 2a, Supplementary Table 1, ICF4). In affected members of family E, we identified a missense mutation in the conserved helicase domain (c.2096A>G;p.[Gln699Arg]) and an intronic mutation leading to destruction of the splice donor site in intron 5 (c.370+2T>A; Fig. 2b). Different allelic origin is supported by analysis of maternal DNA, which carried only the splice site mutation (Fig. 2c). To analyse the effect of the lost splice donor site on mRNA processing, fibroblasts of both patients were treated with cycloheximide to inhibit nonsense-mediated decay. Upon treatment, reverse transcriptase-PCR (RT-PCR) analysis showed increased levels of a splice variant with complete skipping of exon 5, leading to a frameshift followed by a premature stop codon in exon 6 (Fig. 2c).

The patient in family F carries a homozygous out-of-frame deletion (c.2283_2286delGTCT;p.[Ser762Argfs*4]), resulting in a frameshift and introduction of a premature stop codon in exon 20. The unaffected siblings 2.1 and 2.3 were found to be heterozygous for the deletion or homozygous for the wild-type allele, respectively (Fig. 2d). In family G we found a deleterious homozygous in-frame deletion in the C-terminal domain of *HELLS*, leading to the deletion of Leucine 801 (c.2400_2402delGTT;p.[Leu801del]; Fig. 2e). The proband of family H carries a nonsense mutation (c.610A>T;p.[Lys204*]) and a duplication causing the insertion of a stop codon (c.374_381dup;p.[Lys128*]), suggesting that absence of *HELLS* is compatible with human life, whereas *Hells*^{-/-} mice die perinatally¹⁶. Different allelic origin of the mutations was confirmed in parental DNA (Fig. 2f).

ICF genes converge at centromeric DNA methylation regulation.

In mouse, *HELLS* is required for T-cell proliferation and mediates *de novo* DNA methylation, through its interaction with DNMT3B, dependent on its ATPase domain^{16–19}. Genome-wide loss of CpG methylation, including centromeric repeats, has been observed in *Hells*^{-/-} mice, reminiscent of what has been described in *Dnmt3b* knockout mice and in mouse models for ICF1 (refs 20,21). We show that transient depletion of *HELLS*, *CDCA7* and *ZBTB24*, but not DNMT3B, resulted in decreased CpG methylation at centromeric repeats in wild-type mouse embryonic fibroblasts (MEFs, Fig. 2g, Supplementary Fig 3a,b). This confirms that DNMT3B acts during establishment of centromeric CpG methylation²². Moreover, it supports a role for *ZBTB24* and *CDCA7* in maintenance of CpG methylation at centromeric repeats, and, combined with previously published work, suggests that *HELLS* may be involved in both processes¹⁹.

By identifying two new ICF syndrome genes this study highlights the genetic heterogeneity of the syndrome. The identification of at least one additional disease gene is expected with still a few cases remaining genetically unresolved. The complex, but highly overlapping, pathophysiology suggests that all ICF genes act in common or converging pathways involved in

immunity, chromatin regulation and development. Convergence is supported by hypomethylation of pericentromeric repeats, which is common to all ICF subgroups, however the result of different defective pathways in the establishment and/or maintenance of CpG methylation.

Methods

Patients. All samples were obtained in an anonymized manner, and all families gave consent for genetic analyses. The study was approved by the Medical Ethical Committee of the Leiden University Medical Center, the local ethics committee of Necker-Enfants Malades Hospital, Paris, France and the Kyushu University Institutional Review Board for Human Genome/Gene Research. The patient from family A (referred to as patient 2 in ref. 23), patients from families B and C (referred to as pC and pS, respectively, in ref. 12), patient 2.2 from family D and the patients in family E (referred to as P4 and P8/P9 in ref. 5), as well as the three remaining ICFX cases (referred to as pN and P1 in ref. 12 and P4 in ref. 24) all show typical clinical features of ICF syndrome including hypo- or agammaglobulinemia in the presence of B cells, combined with the classical cytogenetic abnormalities involving chromosomes 1, 9 and 16, and hypomethylation of α -satellite DNA in addition to Sat II hypomethylation. The critical features of all patients are summarized in Supplementary Table 1; further details can be found in previous descriptions of these patients^{2,5,6,12,23,24}.

Gene identification by homozygosity mapping and sequencing. Homozygosity mapping was performed using the Sentrix HumanHap-300 Genotyping BeadChips (Illumina). To this end, 750-ng genomic DNA was processed with the Infinium II Whole-Genome Genotyping Assay (Illumina). After DNA amplification, fragmentation, precipitation and resuspension, DNA was applied to the BeadChip and incubated overnight, followed by enzymatic base extension, fluorescent staining of the beads and detection of fluorescent intensities using the BeadArray Reader (Illumina). To identify regions of homozygosity, B allele frequencies were assessed for all single-nucleotide polymorphisms using BeadStudio version 3.2 (Illumina). For a subset of patients, whole-exome sequencing was performed in the Neuroomics project by deCODE Genetics (Reykjavik—Iceland) and analysed using deCODE Clinical Sequence Miner. Recessive analysis for multiple cases and controls and gene variant effect count (with variant effect predictor consequences moderate to high) were used to identify possible recessive mutations. For an additional set of patients, DNA libraries for whole-exome sequencing were constructed using the SureSelect Human All Exon V5 kit (Agilent Technologies) according to the manufacturer's instructions. Sequencing was performed on the Illumina HiSeq2500 platform to generate 100 bp paired-end reads. Reads were mapped to the reference human genome (UCSC hg19) with the Burrows-Wheeler Alignment tool (BWA v0.7.4)²⁵. Duplicate reads were removed by Picard (v1.87). We called SNVs and indels using the Genome Analysis Toolkit (GATK v2.5-2)²⁶. Annotations of variants were made using Annotate Variation (ANNOVAR)²⁷. For confirmation, relevant exons and flanking sequences of *CDCA7* and *HELLS* were amplified using standard PCR; products were purified and analysed using Sanger sequencing. Sequence tracks were analysed and visualized using ContigExpress (Vector NTI, Invitrogen-Life Technologies). PCR primers are listed in Supplementary Table 2.

Cycloheximide treatment and RT-PCR analysis. Early-passage ($P < 6$) patient-derived primary fibroblasts were maintained in DMEM F12 (31331) supplemented with 20% heat-inactivated fetal calf serum, 1% penicillin–streptomycin, 1% sodium pyruvate and 1% HEPES (all Invitrogen-Life Technologies). Cells were treated with 250 $\mu\text{g ml}^{-1}$ cycloheximide (dissolved in ethanol, 01810, Sigma-Aldrich) for 4 h using equal volumes of ethanol as control. After treatment, cells were harvested in Qiazol lysis reagent and RNA was isolated using the miRNeasy mini kit (both Qiagen) all according to the manufacturer's instructions. Total RNA (2 μg) was used for random primed cDNA synthesis using the RevertAid first-strand cDNA synthesis kit (Thermo Scientific). Transcripts were amplified using standard PCR with primers listed in Supplementary Table 2, separated by standard gel electrophoresis and sequenced by Sanger's sequencing.

Knockdown of gene expression in MEFs. The use of animal work has been reviewed by the Animal Experimentation Ethical Committee Buffon (CEEA-40), Paris, France, and was approved under the number CEB-06-2012. Female C57BL/6N pregnant mice, aged 3–6 months, were killed at 12.5 days post conception, and individual MEF clones were isolated from each embryo of the litter. Primary MEFs were cultivated for no more than two to three passages in complete media (DMEM glutamax supplemented with 10% fetal bovine serum, 100 U ml^{-1} penicillin, 100 $\mu\text{g ml}^{-1}$ streptomycin, all from Life Technologies). Two rounds of transfection with synthetic short interfering RNAs (siRNAs) at a final concentration of 20 nM were performed using Interferin transfection reagent (Polyplus transfection) following the manufacturer's instructions: a first round on MEFs in suspension and the second when cells were allowed to adhere to the plate. Cells were collected after 48 h for genomic DNA extraction. Sequences of siRNAs used in the study are listed in Supplementary Table 2.

Satellite DNA methylation analysis using Southern blot analysis. Satellite II and α -satellite methylation in whole-blood DNA was analysed using Southern blot analysis of 2 μ g genomic DNA digested with methylation-sensitive restriction enzymes HhaI for analysis of Sat- α or BstBI for analysis of Satellite II repeats. Both enzymes were purchased from Fermentas. After overnight digestion, DNA was separated by electrophoresis using 0.8% agarose gels. DNA was transferred overnight to Hybond-N+ membranes (GE Healthcare) and hybridized with a radioactive probe recognizing the α -satellite and satellite II repeats, respectively. Signals were detected by phosphorimaging or by exposure to X-ray films. For analysis of murine satellite repeats, genomic DNA was extracted and purified from MEFs using the NucleoSpin Tissue kit (Macherey-Nagel) according to the manufacturer's instructions. The DNA pellet was eluted in Tris EDTA buffer containing 20 μ g ml⁻¹ RNase A. Genomic DNA from MEFs (500 ng) was digested with 20 units of MspI or HpaII (New England Biolabs) for 16 h to analyse the DNA methylation patterns of centromeric minor satellite repeats. The digested DNA fragments were separated by electrophoresis using 1% agarose gels and transferred overnight to Hybond-N+ membranes (GE Healthcare) in 20 \times SSC. After ultraviolet crosslink, the membranes were pre-hybridized in 6 \times SSC, 5 \times Denhardt and 0.1% SDS and then hybridized with 32P-labelled minor satellite oligonucleotide probe: (5'-ACATTCGTTGGAAACGGGATTTGTAGAACAGTG TATATCAATGAGTTACAATGAGAAACAT-3').

Pre-hybridization and hybridization were carried out at 42 °C for 1 h. The membranes were washed three times in 6 \times SSC and 0.1% SDS at 37 °C and signals were detected by phosphorimaging using FLA 7000 phosphorimager (Fuji). Uncropped scans of the Southern blots are presented in Supplementary Figs 4 and 5.

Quantification of knockdown efficiency using qRT-PCR. Total RNA from MEFs was isolated using TRIzol Reagent (Life Technologies) according to the manufacturer's instructions. Contaminant genomic DNA was eliminated with TURBO DNA-free kit (Ambion). Reverse transcription was carried out using 1 μ g DNA-free RNA and 50 μ M random hexamers, 20 U of RNase Out and 100 U of RevertAid reverse transcriptase (Life Technologies). Complementary DNA reactions were used as templates for PCR reactions. Real-time PCR was performed using the light cycler-DNA MasterPLUS SYBR Green I mix (Thermo Scientific) supplemented with 0.5 μ M of specific primer pairs (listed in Supplementary Table 2). Real-time qPCRs were run on a light cycler rapid thermal system (Light Cycler 480 2.0 Real time PCR system, Roche) with 20 s of denaturation at 95 °C, 20 s of annealing at 60 °C and 20 s of extension at 72 °C for all primers, and analysed by the comparative CT (Δ C_t) method.

References

- Hagleitner, M. M. *et al.* Clinical spectrum of immunodeficiency, centromeric instability and facial dysmorphism (ICF syndrome). *J. Med. Genet.* **45**, 93–99 (2008).
- Weemaes, C. M. *et al.* Heterogeneous clinical presentation in ICF syndrome: correlation with underlying gene defects. *Eur. J. Hum. Genet.* **21**, 1219–1225 (2013).
- Jeanpierre, M. *et al.* An embryonic-like methylation pattern of classical satellite DNA is observed in ICF syndrome. *Hum. Mol. Genet.* **2**, 731–735 (1993).
- Tiepolo, L. *et al.* Multibranched chromosomes 1, 9, and 16 in a patient with combined IgA and IgE deficiency. *Hum. Genet.* **51**, 127–137 (1979).
- de Greef, J. C. *et al.* Mutations in ZBTB24 are associated with immunodeficiency, centromeric instability, and facial anomalies syndrome type 2. *Am. J. Hum. Genet.* **88**, 796–804 (2011).
- Jiang, Y. L. *et al.* DNMT3B mutations and DNA methylation defect define two types of ICF syndrome. *Hum. Mutat.* **25**, 56–63 (2005).
- Auclair, G., Guibert, S., Bender, A. & Weber, M. Ontogeny of CpG island methylation and specificity of DNMT3 methyltransferases during embryonic development in the mouse. *Genome Biol.* **15**, 545 (2014).
- Gowher, H. & Jeltsch, A. Molecular enzymology of the catalytic domains of the Dnmt3a and Dnmt3b DNA methyltransferases. *J. Biol. Chem.* **277**, 20409–20414 (2002).
- Moarefi, A. H. & Chedin, F. ICF syndrome mutations cause a broad spectrum of biochemical defects in DNMT3B-mediated *de novo* DNA methylation. *J. Mol. Biol.* **409**, 758–772 (2011).
- Nitta, H. *et al.* Three novel ZBTB24 mutations identified in Japanese and Cape Verdean type 2 ICF syndrome patients. *J. Hum. Genet.* **58**, 455–460 (2013).
- Lee, S. U. & Maeda, T. POK/ZBTB proteins: an emerging family of proteins that regulate lymphoid development and function. *Immunol. Rev.* **247**, 107–119 (2012).
- Velasco, G. *et al.* Germline genes hypomethylation and expression define a molecular signature in peripheral blood of ICF patients: implications for diagnosis and etiology. *Orphanet. J. Rare Dis.* **9**, 56 (2014).
- Gill, R. M., Gabor, T. V., Couzens, A. L. & Scheid, M. P. The MYC-associated protein CDCA7 is phosphorylated by AKT to regulate MYC-dependent apoptosis and transformation. *Mol. Cell Biol.* **33**, 498–513 (2013).
- Guiu, J. *et al.* Identification of Cdca7 as a novel Notch transcriptional target involved in hematopoietic stem cell emergence. *J. Exp. Med.* **211**, 2411–2423 (2014).
- Chen, K., Ou, X. M., Wu, J. B. & Shih, J. C. Transcription factor E2F-associated phosphoprotein (EAPP), RAM2/CDCA7L/JPO2 (R1), and simian virus 40 promoter factor 1 (Sp1) cooperatively regulate glucocorticoid activation of monoamine oxidase B. *Mol. Pharmacol.* **79**, 308–317 (2011).
- Geiman, T. M. & Muegge, K. Lsh, an SNF2/helicase family member, is required for proliferation of mature T lymphocytes. *Proc. Natl Acad. Sci. USA* **97**, 4772–4777 (2000).
- Ren, J. *et al.* The ATP binding site of the chromatin remodeling homolog Lsh is required for nucleosome density and *de novo* DNA methylation at repeat sequences. *Nucleic Acids Res.* **43**, 1444–1455 (2015).
- Yu, W. *et al.* Genome-wide DNA methylation patterns in LSH mutant reveals de-repression of repeat elements and redundant epigenetic silencing pathways. *Genome Res.* **24**, 1613–1623 (2014).
- Zhu, H. *et al.* Lsh is involved in *de novo* methylation of DNA. *EMBO J.* **25**, 335–345 (2006).
- Ueda, Y. *et al.* Roles for Dnmt3b in mammalian development: a mouse model for the ICF syndrome. *Development* **133**, 1183–1192 (2006).
- Velasco, G. *et al.* Dnmt3b recruitment through E2F6 transcriptional repressor mediates germ-line gene silencing in murine somatic tissues. *Proc. Natl Acad. Sci. USA* **107**, 9281–9286 (2010).
- Okano, M., Bell, D. W., Haber, D. A. & Li, E. DNA methyltransferases Dnmt3a and Dnmt3b are essential for *de novo* methylation and mammalian development. *Cell* **99**, 247–257 (1999).
- Kloeckener-Gruissem, B., Betts, D. R., Zankl, A., Berger, W. & Gungor, T. A new and a reclassified ICF patient without mutations in DNMT3B and its interacting proteins SUMO-1 and UBC9. *Am. J. Med. Genet. A* **136**, 31–37 (2005).
- Kubota, T. *et al.* ICF syndrome in a girl with DNA hypomethylation but without detectable DNMT3B mutation. *Am. J. Med. Genet. A* **129A**, 290–293 (2004).
- Li, H. & Durbin, R. Fast and accurate long-read alignment with Burrows-Wheeler transform. *Bioinformatics* **26**, 589–595 (2010).
- McKenna, A. *et al.* The Genome Analysis Toolkit: a MapReduce framework for analyzing next-generation DNA sequencing data. *Genome Res.* **20**, 1297–1303 (2010).
- Wang, K., Li, M. & Hakonarson, H. ANNOVAR: functional annotation of genetic variants from high-throughput sequencing data. *Nucleic Acids Res.* **38**, e164 (2010).

Acknowledgements

We thank all patients and their families for their consent to contribute to our study. We thank K. Ichiyanagi and L. Daxinger for helpful advice, staff of the Kyushu University International Legal Office for help in legal and ethical affairs, and T.P. Pham, S.L. Höcker, M. Miyake and H. Furuumi for technical assistance. This work was supported by KAKENHI (22134006, 23249019 and 26253020), the National Institutes of Health/National Institute of Allergy and Infectious Diseases (R21 AI090135), European Community's Seventh Framework Programme (FP7/2007-2013) under grant agreement no. 2012-305121 'Integrated European—omics research project for diagnosis and therapy in rare neuromuscular and neurodegenerative diseases (NEUROMICS)' and French National Research Agency—Program on physiopathology of rare diseases (ANR-09-GENO-035).

Author contributions

P.E.T., Y.I., G.V., J.W., J.C.d.G., C.W., C.F., S.M.v.d.M. and H.S. conceived and designed the experiments; P.E.T., Y.I., G.G., J.W., G.V., H.N., M.Y., M.S., J.C.d.G., M.M.v.O.-T.D. and M.J.D.v.T. performed the experiments; P.T., Y.I., G.G., J.W., G.V., H.N., M.Y., M.S., Y.S., R.J.L.F.L., J.C.d.G., M.M.v.O.-T.D. and M.J.D.v.T. analysed the data; M.U., A.G., P.P., B.K.-G., T.G., I.R., C.P., K.K., B.R., T.I., T.K., M.M.v.O.-T.D., M.J.D.v.T. and C.W. contributed samples; P.T., C.F., S.M.v.d.M. and H.S. wrote the paper; C.F., S.M.v.d.M. and H.S. jointly supervised the research.

Additional information

Accession Codes: Sequence data have been deposited to the Leiden Open Variation Database (LOVD): <http://databases.lovd.nl/shared/individuals/CDCA7> (IDs CDCA7_000001, CDCA7_000002, CDCA7_000003, CDCA7_000004), <http://databases.lovd.nl/shared/individuals/HELLS> (IDs HELLS_000001, HELLS_000002, HELLS_000003, HELLS_000004, HELLS_000005, HELLS_000006).

Supplementary Information accompanies this paper at <http://www.nature.com/naturecommunications>

Competing financial interests: The authors declare no competing financial interests.

Reprints and permission information is available online at <http://npg.nature.com/reprintsandpermissions/>

How to cite this article: Thijssen, P. E. *et al.* Mutations in *CDCA7* and *HELLS* cause immunodeficiency–centromeric instability–facial anomalies syndrome. *Nat. Commun.* 6:7870 doi: 10.1038/ncomms8870 (2015).



This work is licensed under a Creative Commons Attribution 4.0 International License. The images or other third party material in this article are included in the article's Creative Commons license, unless indicated otherwise in the credit line; if the material is not included under the Creative Commons license, users will need to obtain permission from the license holder to reproduce the material. To view a copy of this license, visit <http://creativecommons.org/licenses/by/4.0/>

Corrigendum: Mutations in *CDCA7* and *HELLS* cause immunodeficiency-centromeric instability-facial anomalies syndrome

Peter E. Thijssen, Yuya Ito, Giacomo Grillo, Jun Wang, Guillaume Velasco, Hirohisa Nitta, Motoko Unoki, Minako Yoshihara, Mikita Suyama, Yu Sun, Richard J.L.F. Lemmers, Jessica C. de Greef, Andrew Gennery, Paolo Picco, Barbara Kloeckener-Gruissem, Tayfun Güngör, Ismail Reisli, Capucine Picard, Kamila Kebaili, Bertrand Roquelaure, Tsuyako Iwai, Ikuko Kondo, Takeo Kubota, Monique M. van Ostaijen-Ten Dam, Maarten J.D. van Tol, Corry Weemaes, Claire Francastel, Silvère M. van der Maarel & Hiroyuki Sasaki

Nature Communications 6:7870 doi: 10.1038/ncomms8870 (2015); Published 28 Jul 2015; Updated 22 Jun 2016

In Fig. 1b of this Article, the sex of patient 2.1 in family A is incorrect, and should be depicted as male. The correct version of this figure appears below.

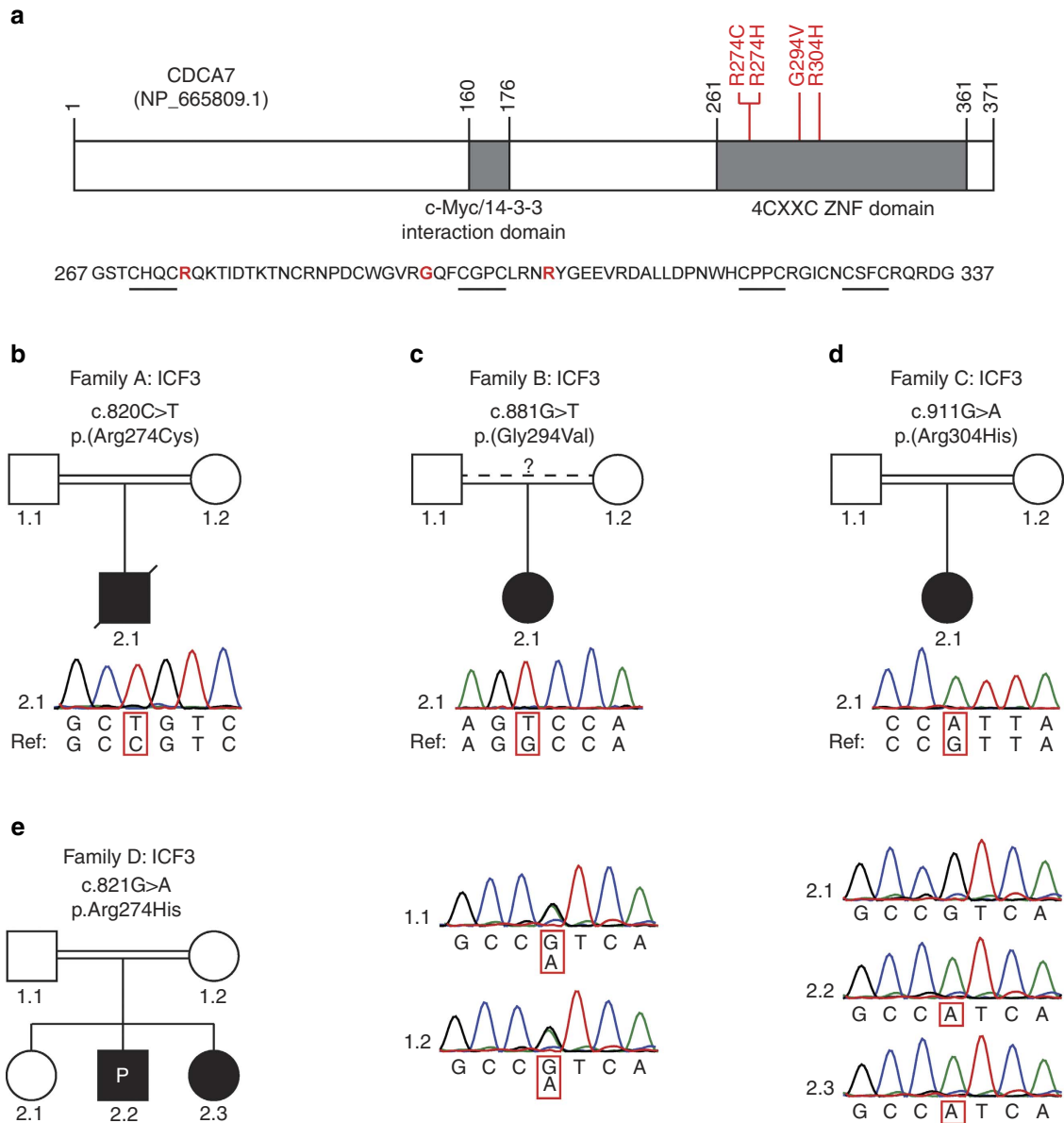


Figure 1

This work is licensed under a Creative Commons Attribution 4.0 International License. The images or other third party material in this article are included in the article's Creative Commons license, unless indicated otherwise in the credit line; if the material is not included under the Creative Commons license, users will need to obtain permission from the license holder to reproduce the material. To view a copy of this license, visit <http://creativecommons.org/licenses/by/4.0/>